Nonequilibrium supercurrent transport in controllable superconductor–normal-metal–superconductor junctions

J. J. A. Baselmans,[1] B. J. van Wees,[1] and T. M. Klapwijk[2]
[1]*Department of Applied Physics and Materials Science Center, University of Groningen, Nijenborg 4, 9747 AG Groningen, The Netherlands*
[2]*Department of Applied Physics and DIMES, Delft University of Technology, Lorentzweg 1, 2628 CJ Delft, The Netherlands*
(Received 12 July 2000; published 30 January 2001)

We study the supercurrent through a superconductor (Nb)–normal-metal (Ti-Au bilayer)–superconductor junction as a function of the electron distribution in the normal region. The normal region of the junction is coupled to the center of a mesoscopic wire (control channel) over which a control voltage V_c can be applied. The effective electron-electron relaxation in the wire determines the shape of the electron distribution and therefore the critical current of the SNS junction. For a short (1 μm) control channel we observe the transition to a π state of the junction whereas for a junction with a long (9 μm) control channel we observe a monotonic decrease of the critical current. The data are in good quantitative agreement with theory at higher energies, but at low energies important geometry dependent deviations arise. The inferred electron-electron interaction time in the normal metal τ_{e-e} equals 10 ps.

DOI: 10.1103/PhysRevB.63.094504 PACS number(s): 74.50.+r, 73.23.−b, 85.25.Am, 85.25.Cp

I. INTRODUCTION

The fundamental process which enables supercurrent transport through a superconductor–normal-metal–superconductor (SNS) junction is Andreev reflection. In a ballistic junction, in which the elastic mean-free path in the normal region is longer than the length l of the normal metal, discrete Andreev bound states are formed which carry the supercurrent.[1–3] In a junction in which the elastic mean-free path is much shorter than the length of the normal region the electron motion is diffusive and a discrete spectrum of states is no longer the appropiate concept to describe the supercurrent. In these systems the supercurrent is carried by a continuous density of states,[4–7] which depends on the junction geometry. The maximum supercurrent in such a SNS junction depends on the occupation of the supercurrent carrying states. By changing the electron distribution function in the normal region it has been shown experimentally[8,9] that it is possible to suppress the critical current, or even reverse[10,11] its direction with respect to the phase difference between the superconducting electrodes, corresponding to the transition to a π junction.

In this paper we compare *quantitatively* the theoretical dependence of the supercurrent on the shape of the electron distribution to the experiment. The device used is shown in Fig. 1. A narrow diffusive gold wire (control channel), which has two extensions in its center, is connected to large electron reservoirs (gold). The extensions are covered partly by niobium superconductors, thus forming a very narrow SNS junction in the center of the control channel. The distribution of the electrons over the energy in the normal region of the junction depends on the voltage V_c applied over the control channel and on the amount of electron-electron scattering in the channel (at the measuring temperatures one can ignore electron-phonon interactions). If the channel is short, so that the electron-electron interaction time τ_0 exceeds the diffusion time τ_D, the electrons will conserve their energy and the electron distribution will be the superposition of the distribution functions of the reservoirs, of which the chemical potentials will be shifted by a value eV_c. If $k_bT<eV_c$ it will show a double step structure, with a separation of eV_c between the steps. If the wire is long, so that $\tau_D \gg \tau_0$, the distribution function will be a thermal one, with an effective temperature $T_{eff} \geqslant T_B$ depending on V_c.[12] The value of T_{eff} is determined by the ratio of the heating in the wire and the thermal conductance to the reservoirs which, using the Wiedemann-Franz law, leads to:

$$T_{eff}=\sqrt{T_{e,res}{}^2+(a\cdot V_c)^2}, \tag{1}$$

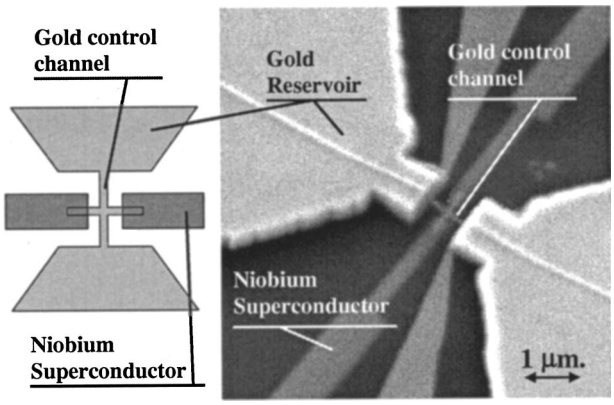

FIG. 1. Scanning electron microscope picture of one of the devices (right) as well as a schematic drawing of the device structure (left). A narrow (100 nm) gold channel, which has two side arms in its center, is connected to large electron reservoirs. The side arms are covered partly by niobium electrodes, thus forming a very narrow (100 nm) SNS junction in the center of the channel. In the figure the control channel length is 1 μm, but devices with a long control channel (9 μm) have also been studied.

with a=3.2 K/mV in the center of the wire[12] and $T_{e,res}$ the electron temperature in the reservoirs equal to the bath temperature T_B for perfect reservoirs.

The devices are fabricated in three steps on a thermally oxidized Si wafer by means of conventional *e*-beam lithography with PMMA resist. The control channel, consisting of 5 nm Ti (to improve adhesion) and 40 nm Au was deposited first using electron-beam evaporation. In two subsequent steps the niobium (70 nm) was sputter deposited and the reservoirs (5 nm Ti and 475 nm of Au) were deposited. Prior to these two steps we used an *in situ* Ar etching to ensure a high interface transparency. The reservoirs have to be both very thick and very large because they should also act as effective cooling fins to prevent unwanted electron heating.[13,14] We studied three different device geometries. Device 1 (two identical devices measured) with a length of the control channel L=1 μm, Device 2 (two identical devices measured) with $L=9$ μm, and the device measured in Ref. 10 which we call Device 3. The behavior of identical devices is similar, so we present only the data of one of them in the remainder of the article. Devices 1 and 2 are made in the same batch and are geometrically identical, except for the length of the control channel. The width of the control channel as well as the width of the wire which forms the normal region of the SNS juntion is 100 nm. The distance between the Nb electrodes is 375 nm and the total length of the normal region of SNS junction (which is partly covered by the Nb) is 1 μm. The central region of Devices 1 and 2 is therefore a perfect cross wire with 100 nm wide leads. The diffusion coefficient $D=0.020$ m^2/s (obtained using the measured square resistance) which results in an estimated diffusion time through the channel of $\tau_D=50$ ps and 4 ns for Devices 1 and 2, respectively. The SNS junctions of these Devices have an identical normal-state resistances of 2.1 Ω and Device 1 has a control channel resistance of $R_{control}=4.4$ Ω, whereas Device 2 has a control channel resistance of $R_{control}=39$ Ω. Device 3 is made in an earlier batch and the width of the SNS junction is 400 nm, the distance between the Nb electrodes is 300 nm and the total length of the normal region of the SNS junction (which is partly covered by the Nb) is 1.2 μm. The width of the control channel is 200 nm and the length is 700 nm. The normal state resistance of he junction is 0.75 Ω, $R_{control}=1.5\Omega$. The diffusion coefficient $D=0.018$ m^2/s (obtained using the measured square resistance) which results in an estimated diffusion time through the channel of $\tau_D=27$ ps. The thickness of the Nb, gold wires, gold reservoirs, and the Ti adhesion layer are identical for all three devices

II. THEORY

The dependence of the critical current of a SNS junction I_c (critical current times normal-state resistance) on the exact shape of the electron distribution can be calculated if the exact spectrum of the supercurrent carrying states, Im$[J(\epsilon)]$, is known. For a diffusive system, this will be a continuous function of energy, which is a result from the phase coherent transport of electron-hole pairs in the normal region. The supercurrent can be calculated according to[4–7]

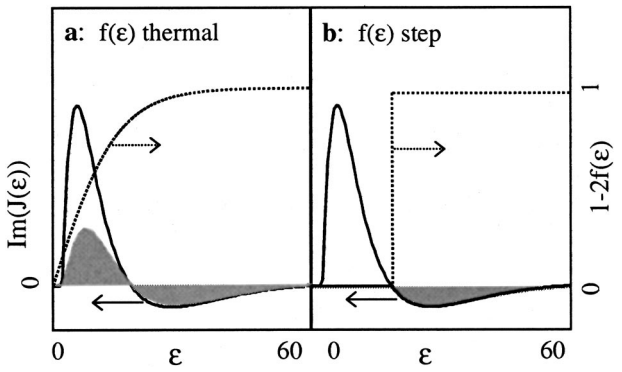

FIG. 2. Supercurrent carrying density of states Im$[J(\epsilon)]$ for $\Delta/E_{th}=70$ at $\phi=\pi/2$ (solid line) together with $1-2f(\epsilon)$ (dotted line) in the case of a thermal distribution (a), and a step distribution (b). The shaded area represents the integrand of Eq. (2). ϵ represents the energy normalized to E_{th}.

$$I_c=\frac{1}{R_n}\int_{-\infty}^{\infty} d\epsilon[1-2f(\epsilon)]\mathrm{Im}[J(\epsilon,\phi=\pi/2)], \qquad (2)$$

where ϕ the phase difference between the superconducting electrodes,[15] ϵ is the energy normalized to the Thouless energy $E_{th}=\hbar D/l^2$, $f(\epsilon)$ the electron distribution function and R_n the normal-state resistance of the junction, given by $(\sigma_n W)/l$ with W the junction width and σ_n the conductivity of the normal metal. It should be pointed out that the exact amplitude of the supercurrent does differ between the different theoretical papers[4–7] and a more recent prediction[16] gives a lower value than in Ref. 6. The exact shape of Im$[J(\epsilon)]$ depends on the ratio of the Thouless energy with the energy gap Δ of the superconductors and is calculated using the quasiclassical Green's function theory.[4–7] The general shape of Im$[J(\epsilon)]$, as shown in Fig. 2 is a strongly damped oscillation with a hard gap at low energies $E \lesssim E_{th}$. The positive and negative parts of the supercurrent carrying density of states represent energy dependent contributions to the supercurrent in the positive and negative direction. A thermal distribution in *N* results, as shown in Fig. 2(a), in a rapid decay of the supercurrent with increasing temperatures due to the compensation of the positive and negative contributions in Im$[J(\epsilon)]$. A step distribution will, at a large enough value of V_c, block all the positive contributions to the supercurrent, as shown in Fig. 2(b), which gives rise to a reversal in the direction of the supercurrent.

It is important to realize that the calculation of Im$[J(\epsilon)]$ is done in a one-dimensional (1D) wire geometry, so it is to be expected that the exact shape of Im$[J(\epsilon)]$ changes if reservoirs are coupled to the system by means of clean contacts. Qualitatively the deviations from the theoretical 1D case in the situation of a realistic device are the following: (1) A reduction of the overall amplitude of Im$[J(\epsilon)]$, caused by electrons coming from the reservoir which can Andreev reflect on one of the superconductors and leave again to the reservoirs. This effect scales with the conductance of the control channel relative to the normal-state conductance of the SNS junction. (2) A smearing out of the hard gap at low energies of Im$[J(\epsilon)]$, due to a finite dwell time of electrons

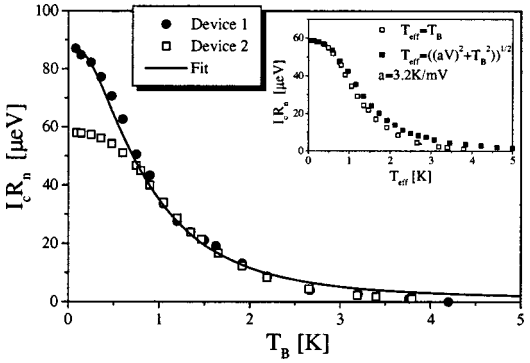

FIG. 3. I_c of both devices as a function of the bath temperature T_B, together with a fit, obtained by using a Fermi-Dirac distribution at T_B. The inset shows the data of Device 2, as a function of T_B ($V_c=0$) and V_c ($T_B=100$ mK) expressed as an effective temperature T_{eff} using the Wiedeman-Franz law.

in the normal region of the junction. (3) An overall change in the shape of $\mathrm{Im}[J(\epsilon)]$ due to a different distribution of the length of the paths which are traveled by phase coherent electron-hole pairs between the two superconducting electrodes. This effect is stronger if the wire connecting the reservoir to the normal region of the junction is longer, for a quasiparticle entering the wire will have a larger probability of returning to the normal region of the junction instead of escaping to the reservoir. In this case more paths with a greater length will be present compared to the quasi-1D wire geometry, resulting in a decrease in the effective Thouless energy of the junction.

From these arguments it is clear that $\mathrm{Im}[J(\epsilon)]$ is expected to be geometry dependent due to the presence of the control channel and the normal reservoirs. This is demonstrated by Yip,[7] who calculated $\mathrm{Im}[J(\epsilon)]$ for a symmetrical four-terminal junction, in which the wires to the superconductors and the reservoirs are all equal in length and equal in resistance. In this limit he finds an overall reduction of magnitude of $\mathrm{Im}[J(\epsilon)]$ and a change in its shape only at low energies $E<E_{th}$, which is consistent with the above arguments.

III. EXPERIMENT

In the experiment we measure the current-voltage (I-V) characteristics of the SNS junction as a function of the voltage V_c applied over the control channel at a bath temperature $T_B=100$ mK. We also measure the I-V characteristics of the junction as a function of T_B with $V_c=0$ V. From these measurements we obtain the critical current both as a function of T_B and V_c. The direction of the supercurrent is determined by measuring the modulation of the resistance of the control channel as a function of the current bias through the SNS junction (for details see Ref. 10). In Fig. 3 we show the results as a function of T_B. The critical current I_c, for normalization purposes multiplied with the normal-state resistance of the junction R_n, of both devices decays rapidly with increasing T_B. This is in qualitative agreement with theory. Moreover, at $T_B>0.8$ K both curves fall exactly on top of each other, consistent with the fact that both junctions are geometrically identical except for the length of the control channel. The supercurrent in the case of Device 2 saturates at lower temperatures, resulting in a much lower critical current at $T_B=100$ mK. The inset of the Fig. 3 reproduces the data of Device 2, together with I_c as a function of V_c ($T_B=100$ mK), in which V_c is expressed as an effective temperature T_{eff} using Eq. 1 and the theoretical value of $a=3.2$ K/mV. Both curves fall essentially on top of each other at $T<1$ K, but the voltage controlled experiment yields a somewhat larger supercurrent (and hence a lower effective temperature than calculated) at higher temperatures. This difference could be caused by electron-phonon scattering in the long control channel of Device 2, for $\tau_{e-ph}\lesssim 1$ nsec for similar gold wires[17] at $T>1$ K. Incomplete thermalization of the electrons in the wire, indicating that the condition $\tau_{e-e}\ll\tau_D$ is not applicable, or reservoir heating, are no suitable candidates for the observed difference between the measurements. These effects would yield a higher effective electron temperature and thus a lower supercurrent in the voltage controlled case, as in Ref. 8.

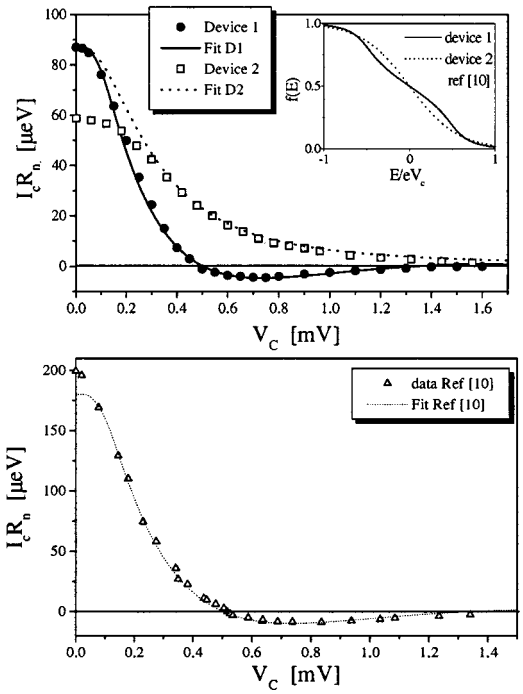

FIG. 4. The top panel shows I_c of Devices 1 and 2 as a function of V_c ($T_B=100$ mK). The bottom figure shows the data Device 3 (reproduced from Ref. 10). The lines represent the best fits to the theory using the same fit parameters for all devices, except for the zero voltage critical current. The inset shows the corresponding distribution functions in the center of the control channel.

The top panel of Fig. 4 shows I_c of Devices 1 and 2 as a function of the control voltage. In the bottom panel we show the data from Device 3. The data of Devices 1 and 3 show the transition to a π junction at $V_c>0.5$ meV, which clearly signals that the distribution function in the normal region is nonthermal. It also indicates that the Thouless energy of both devices should be identical, for the location of the transition to the π state is determined by the energy range of $\mathrm{Im}[J(\epsilon)]$. The data of Device 2 decay rapidly with increasing V_c, consistent with a thermal distribution function, with an effective

electron temperature $T_{eff} > T_B$ as shown in the inset of Fig. 3. Both observations are in qualitative agreement with theory. However, the maximum critical current in the π state is much smaller than predicted for a perfect steplike distribution.

IV. DISCUSSION

The next step in our analysis is a quantitative comparison between the experimental data and the theory. We start with the temperature-dependent data. In this case the shape of the electron distribution is known and $\mathrm{Im}[J(\epsilon)]$ can be calculated. We stress that this calculation was done in a 1D geometry. The best fit, shown by the line in Fig. 3, uses a thermal distribution with $T = T_B$ and $E_{th} = 21\ \mu\mathrm{eV}$ for both devices and $I_{c,0}R_n = 87\ \mu\mathrm{eV} = 4.1E_{th}$ ($I_{c,0}$ is the maximum critical current at $T_B = 100$ mK and $V_c = 0$). The effective Nb electrode separation using this value of E_{th} yields l=800 nm, which is in between the minimum Nb separation and the maximum extent of the gold under the Nb (1 μm). The fit to the data is excellent, except for the low-temperature region of Device 2. An improved fit of these data, by an adjustment of $I_{c,0}R_n$ a change in Thouless energy could not be obtained. We conclude therefore that the predicted 1D form of $\mathrm{Im}[J(\epsilon)]$ is in agreement with the observed supercurrent vs temperature behavior of Device 1, and with Device 2 at higher energies. Moreover, the absolute value of the $I_{c,0}R_n$ product of Device 2, $87\ \mu\mathrm{eV} = 4.1E_{th}$, is in reasonable agreement with theory. It is predicted that[7] $I_{c,0}R_n = 5E_{th} = 105\ \mu\mathrm{eV}$ for a perfectly symmetric device (length and surface area of the wires to both the normal reservoirs as well as the superconductors being identical).

To be able to fit the data of the V_c controlled experiment we have to calculate the shape of the distribution function as a function of V_c, which was done using the method described in Ref. 12. In this model the shape of the distribution function depends on two parameters: The ratio τ_0/τ_D, which represents the effective electron, electron interaction in the wire, and $kT_{e,res}/eV_c$, where $T_{e,res}$ is the electron temperature in the reservoirs close to the control channel, not to be confused with T_{eff}. $T_{e,res}$ cannot be taken as a constant and equal to T_B, because the electron heat conductance of the reservoirs is finite and because the electron-phonon interaction is strongly reduced at low temperatures. These arguments combined with the fact that rather large control voltages are used in these experiments make it necessary to calculate the heating of the electrons in the reservoirs explicitly. We calculated the value of $kT_{e,res}/eV_c$ for every measured data point using a model presented by Welstood[13] and Henny *et al.*[14] The result is that, at $T_B = 100$ mK, $T_{e,res}$ increases with increasing control voltage. This increase becomes linear for $V_c > 0.4$ mV. In this limit $kT_{e,res}/eV_c$ is a constant, which implies that the shape of the distribution function is also constant. Higher values of the applied voltage merely change the energy range of the distribution function, not its shape.[12] The results of the fits are shown by the lines in Fig. 4. We find $E_{th} = 21\ \mu\mathrm{eV}$ for all devices, and a value of $I_{c,0}R_n = 87\ \mu\mathrm{eV} = 4E_{th}$ for Devices 1 and 2. For Device 3 we find $I_{c,0}R_n = 180\mu\ \mathrm{eV} = 8.6E_{th}$, which is larger than expected for a cross geometry ($5E_{th}$), but smaller than the value expected for a 1D system ($10.8E_{th}$).[16] The electron distributions used for the fits are shown in the inset of the top panel, in the limit that $kT_{e,res}/eV_c = \text{constant}$. It is clear that the agreement between the experiment and the calculations is excellent, apart from the low voltage region of Device 2. However, from the inserts it is also clear that *the shape of the distribution functions indicates a significant electron-electron interaction*: The distribution function has a Fermi-Dirac shape in the case of Device 2, which was expected, but it is *also very rounded already in the case of Devices 1 and 3*. The interaction time constant τ_0 obtained from this analysis is given by $\tau_0 \approx 10$ ps for Devices 1 and 2 and $\tau_0 \approx 5$ ps. for Device 3. The value of τ_0 can be compared to the theoretical electron-electron interaction time τ_{e-e}, for it implies an upper bound for the quasiparticle lifetime (see Ref. 12) $\tau_{qp} = 10$ ps. (which at these temperatures should be identical to τ_{e-e}), valid over the energy range of these experiments (0.01–1.8 meV). τ_{e-e} can be calculated using the material independent theory on electron-electron interactions in a diffusive 1D wire, according to[18–20]

$$\tau_{e-e}(E) = \sqrt{2}\hbar n_0 S \sqrt{\frac{\hbar D}{E}}, \tag{3}$$

with n_0 the density of states at the Fermi level in *N*, and *S* the area cross-section area of the wire. This yields, using $n_0 = 1.9 \cdot 10^{28}\ \mathrm{m}^{-3}\mathrm{eV}^{-1}$ $\tau_{ee}(0.01\ \mathrm{meV}) = 80$ ns, a difference of at least four orders of magnitude with our inferred result. We wish to emphasize that our referred value depends only weakly on the exact fit parameters and is determined by the relative size of the π supercurrent alone as shown in the top panel of Fig. 5. There we show the theoretical dependence of I_c on the control voltage for different values of the effective electron interaction in the control channel, τ_0/τ_D. It is clear that, if $0.1 < \tau_0/\tau_D < 1$, τ_0/τ_D is determined only by the ratio of the maximum supercurrent in the π state with the equilibrium supercurrent, $I_{c,\pi max}/I_{c,0}$. An increase of τ_0 of only a factor of 5 would already result in $I_{c,\pi max}/I_{c,0} \approx 0.3$ for Device 1, being the value obtained if the distribution would be perfectly steplike. From Fig. 5 it is also clear that for $\tau_0 \geqslant 0.8$ nsec. Device 2 would show a transition to a π state. This indicates that value of τ_{e-e} obtained using Eq. (3) is in clear disagreement with the observations. We note that experiments on similar wires using a direct measurement of the distribution function with superconducting tunnel junctions[21] give a value of $\tau_0 = 100$ ps for gold. Recently experimental[21] and theoretical[23,22] developments strongly indicate that τ_{e-e} might be less universal than suggested by Eq. (3), but strongly dependent on the material and the exact process used to fabricate the sample. So there is reason to assume that the difference of a factor of 10 between our data and these measurements is related to the fact that we used a different fabrication process. This also explains the difference in τ_0 between Devices 1 and 3, which were made in different batches. The fact that Ti is a superconductor with $T_c = 0.39$ K should not play a role, because the layer thickness of the Ti, 5 nm, is much smaller than the estimated

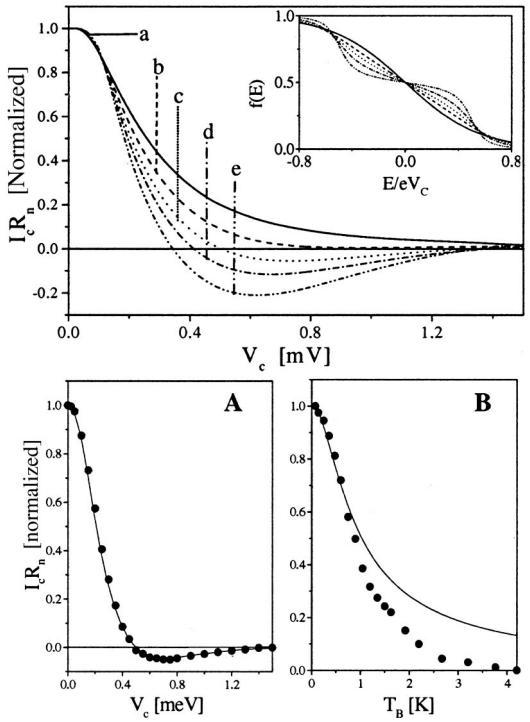

FIG. 5. The top figure shows the theoretical dependence of the I_cR_n vs V_c behavior on the effective electron-electron interaction in the control channel, τ_0/τ_D. The inset shows the corresponding distribution functions. $\tau_0/\tau_D=$: **a**: 0, **b**: 0.1, **c**: 0.2, **d**: 0.4, **e**: 1. $\tau_d=50$ ps and 4 ns for Devices 1 and 2, respectively. The two bottom figures show a theoretical fit to both the V_c and T_B dependence of Device 1, assuming a perfect step distribution function and a smaller negative contribution in Im$[J(\epsilon)]$. It is obvious that a consistent fit is not possible in this case.

coherence length, yielding a strong suppression of T_c due to the presence of the 40 nm gold layer.

The first remaining question is whether it is not possible to obtain a good agreement between theory and experiment using a larger value for τ_0. This implies a perfect double step distribution function for Device 1, which can only be possible if Im$[J(\epsilon)]$ differs strongly from the calculated form. Assuming such a perfect double step distribution in Device 1, it is possible to find a form of Im$[J(\epsilon)]$ such that the fit with the voltage dependent data of Device 1 is excellent [see Fig. 5(a)]. However, using this form of Im$[J(\epsilon)]$ results in a fit to the temperature-dependent data as shown by the line in Fig. 5(b). The very slow decrease in supercurrent clearly contradicts all data. These arguments indicate directly that the shape of Im$[J(\epsilon)]$ as calculated in Refs. 4–7 is in principle correct, because a consistent fit for both the V_c and T_B dependent is otherwise not possible and that a very rounded electron distribution alone is responsible for the small values of the π supercurrent.

Another point is the observed differences between the devices and the quality of the fits. The good fit of the data of Devices 1 and 3 implies that the quasi-1D theoretical form of Im$[J(\epsilon)]$ is applicable to these devices, however, a difference in amplitude is needed, because Device 1 has a lower-value of $I_{c,0}R_n/E_{th}$. The low-energy region of Device 2 deviates from the theoretical behavior. The supercurrent saturates and shows a large region over which it is only very weakly dependent on energy. As discussed previously, there are three possible deviations in our samples from a 1D theory: A noninfinite dwell time of electrons, which causes a smearing in the hard gap in Im$[J(\epsilon)]$, the influence from quasiparticles coming from the reservoirs, which reduces the amplitude of Im$[J(\epsilon)]$, and the distribution of possible paths of phase coherent electron-hole pairs, which will change the effective Thouless energy. We would like to stress that the last effect might cause the observed differences between the devices. To do this we will first explain why the other two effects can be ignored. The first point is that the good fit of Device 1 indicates that the 1D form of Im$[J(\epsilon)]$ applies, indicating that the gap smearing is not observable for Device 1 (The effect of the smearing of the gap is weakly observed in Device 3, as can be seen by the first two data points in Fig. 4). This implies that, because the 1D theory gives an upper bound of the gap size, that the behavior of Device 2 at low energies cannot be explained by a larger gap in Im$[J(\epsilon)]$. This is consistent with the fact that no fit could be obtained for this data at low energies. The second point is that the observed difference in $I_{c,0}R_n/E_{th}$ between Devices 1 and 3 cannot be explained by a difference in influence of the reservoirs. The reason is that the conduction of the control channel relative to the conduction in the normal state of the SNS junction is identical for both devices, so the influence of the reservoirs will be identical. Moreover, the effect of the reservoir is strongest in the Device 3, which would cause a lower value of $I_{c,0}R_n/E_{th}$ in this case than for Device 1, which is not observed. These points combined indicate that the distribution of possible paths of phase coherent electron-hole pairs between the superconducting electrodes should be responsible for the observed differences between the devices. The geometries of the devices are the following: Device 3 has a wide SNS junction with relative narrow and short control channel. So the paths possible between the superconducting electrodes differ only weakly from a true wire geometry as assumed in the theoretical papers. This is consistent with the observation that $I_{c,0}R_n/E_{th}=8.6$, which is relatively close to the predicted 1D value of 10.6. Device 1 has a geometry which is close to a perfect cross, the control channel and normal region of the junction are both 100 nm wide and differ only on length. The value of $I_{c,0}R_n/E_{th}=4$ whereas the prediction is that if the normal region of the SNS junction and the control channel are identical $I_{c,0}R_n/E_{th}=5$. The saturation of the supercurrent of Device 2 at lower temperatures might be explained qualitatively using a simular argument. If the temperature decreases the phase coherence length l_ϕ increases which indicates that the phase coherent electron-hole paths can extend over longer region, especially in the long control channel of Device 2. The difference with a 1D device is a larger fraction of longer pathways, which reduces the effective Thouless energy of the SNS junction and hence causes a saturation of the critical current at lower temperatures. The fact that the critical currents of Devices 1 and 2 are identical at $T_B>0.8$ K indicates that in this limit the l_ϕ should be in the order or less than the length of the control channel of Device 1, implying $\tau_\phi \approx \tau_D=50$ ps. at

0.8 K. This value is consistent with magnetoresistance experiments on similar gold films.[17]

V. CONCLUSION

We conclude that the theoretical (quasi-1D) description of supercurrent transport in diffusive SNS junctions as a function of the electron distribution is accurate. The calculated form of the supercurrent carrying density of states is the only form which explains the temperature dependence as well as the voltage dependence of the supercurrent consistently. Thus the small value of the π supercurrent is caused by a very fast electron-electron interaction time constant $\tau_0 = 10$ ps in the Ti-Au control channel. The exact value of τ_0 is found to be determined within a factor of 3 by the relative magnitude of the π supercurrent alone and is therefore only weakly dependent on the fit. The value is about a factor of 10 smaller than other measurements on gold wires but the difference between our referred value of τ_0 and the conventional theoretical prediction, using Eq. (3), is at least four orders of magnitude. This difference might be accounted for by the fact that recent insights indicate that the strength of the electron-electron relaxation is strongly material dependent as well as very sensitive to the exact fabrication procedures, which vary from system to system. The observed geometry dependence of the supercurrent, especially the low-energy region of Device 2, can be qualitatively discussed in terms of geometrical effects. A full 2D theoretical description of supercurrent transport in multiterminal devices such as used in these experiments is needed to verify these assumptions.

ACKNOWLEDGMENTS

We gratefully acknowledge H. Pothier and F. K. Wilhelm for making their computer programs available to us. Furthermore we thank A. F. Morpurgo for his initiating role leading to this work. This work was supported by the Nederlandse Organisatie voor Wetenschappelijk Onderzoek (NWO) through the Stichting voor Fundamenteel Onderzoek der Materie (FOM).

[1] I.O. Kulik, Zh. Éksp. Teor. Fiz. **57**, 1745 (1969) [Sov. Phys. JETP **30**, 944 (1970)].
[2] C. Ishii, Prog. Theor. Phys. **5**, 1525 (1972).
[3] J. Bardeen and J.L. Johnsen, Phys. Rev. B **5**, 72 (1972).
[4] A.F. Volkov, Phys. Rev. Lett. **74**, 4730 (1995).
[5] A.F. Volkov and H. Takayanagi, Phys. Rev. B **56**, 11 184 (1997).
[6] F.K. Wilhelm, G. Schön, and A.D. Zaikin, Phys. Rev. Lett. **81**, 1682 (1998).
[7] S.-K Yip, Phys. Rev. B **58**, 5803 (1998).
[8] A.F. Morpurgo, T.M. Klapwijk, and B.J. van Wees, Appl. Phys. Lett. **72**, 966 (1998).
[9] K. Neurohr, Th. Schäpers, J. Malindretos, S. Lachenmann, A.I. Braginski, H. Lüth, M. Behet, G. Borghs, and A.A. Golubov, Phys. Rev. B **59**, 11 197 (1999).
[10] J.J.A. Baselmans, A.F. Morpurgo, B.J. van Wees, and T.M. Klapwijk, Nature (London) **397**, 43 (1999).
[11] R. Shaikhaidarov, A.F. Volkov, H. Takayanagi, V.T. Petrashov, and P Delsing, cond-mat/0010144, Phys. Rev. B (to be published 1 December 2000).
[12] H. Pothier, S. Guéron, N.O. Birge, D. Esteve, and M.H. Devoret, Phys. Rev. Lett. **79**, 3490 (1997).
[13] F.C. Wellstood, C. Urbina, and J. Clarke, Phys. Rev. B **49**, 5942 (1994).
[14] M. Henny, S. Oberholzer, C. Strunk, and C. Schönenberger, Phys. Rev. B **59**, 2871 (1999).
[15] We have used the fact that the critical current generally equals the supercurrent if the phase difference is $\pi/2$. This is not fully correct, but only leads to minor changes in the calculated curves (Refs. 6 and 7).
[16] P. Dubos, H. Courtois, B. Pannetier, F.K. Wilhelm, A.D. Zaikin, and G. Schön, Phys. Rev. B **63**, 064502 (2000).
[17] P. Mohanty, E.M.Q. Jariwala, and R.A. Webb, Phys. Rev. Lett. **78**, 3366 (1997).
[18] A. Schmidt, Z. Phys. **271**, 251 (1974).
[19] B.L. Altshuler, A.G. Aronov, Zh. Éksp. Teor. Fiz **75**, 1610 (1978) [Sov. Phys. JETP **48**, 812 (1978)].
[20] B.L. Altshuler and A.G. Aronov, in *Electron-Electron interactions in Disordered Systems*, edited by A.L. Efros and M. Pollak (North-Holland, Amsterdam, 1985).
[21] F. Pierre, H. Pothier, D. Estève, and M.H. Devoret, J. Low Temp. Phys. **118**, 437 (2000).
[22] Y. Imry, H. Fukuyama, and P. Schwab, Europhys. Lett. **47**, 608 (1999).
[23] A. Zawadowski, Jan von Delft, D.C. Ralph, Phys. Rev. Lett. **83**, 2632 (1999).